THE UNIVERSITY OF

WARWICK

University of Warwick institutional repository: http://go.warwick.ac.uk/wrap

This paper is made available online in accordance with
publisher policies. Please scroll down to view the document
itself. Please refer to the repository record for this item and our
policy information available from the repository home page for
further information.

To see the final version of this paper please visit the publisher's website.
Access to the published version may require a subscription.

Author(s): A. Chaudhuria, T.J. Lerotholia, D.C. Jacksona, D.P.
Woodruffa, , and V.R. Dhanak
Article Title: The local adsorption structure of methylthiolate and
butylthiolate on Au(1 1 1): A photoemission core-level shift investigation
Year of publication: 2009
Link to published version:
 http://dx.doi.org/10.1016/j.susc.2009.11.010
Publisher statement: None

The local adsorption structure of methylthiolate and butylthiolate on Au(111): a photoemission core-level shift investigation

A. Chaudhuri, T.J. Lerotholi, D.C. Jackson, D.P. Woodruff[*]
Physics Department, University of Warwick, Coventry CV4 7AL, UK
V.R. Dhanak
Surface Science Research Centre, University of Liverpool and Daresbury Laboratory,
Warrington WA4 4AD, UK

Abstract

Measurements of the core level shifts in Au 4f photoemission spectra from Au(111) at different coverages of methylthiolate and butylthiolate are reported. Adsorption leads to two components in addition to that from the bulk, one at lower photoelectron binding energy attributed to surface atoms not bonded to thiolate species, while the second component has a higher binding energy and is attributed to Au atoms bonded to the surface thiolate. The relative intensities of these surface components for the saturation coverage (mainly ($\sqrt{3}$x$\sqrt{3}$)R30°) phases are discussed in terms of different local adsorption sites in a well-ordered surface, and favour adsorption of the thiolate species atop Au adatoms. Alternative interpretations that might be consistent with an Au-adatom-dithiolate model are discussed, particularly in the context of the possible influence of reduced coverage associated with a disordered surface. Marked differences from previously-reported results for longer-chain alkylthiolate layers are highlighted.

keywords: chemisorption; self-assembly; gold; thiols

---

[*] corresponding author, email D.P.Woodruff@warwick.ac.uk

1. Introduction

Despite the many investigations of alkylthiolates ($CH_3(CH_2)_{n-1}S$) adsorbed on Au(111) to produce so-called self-assembled monolayers (SAMs) (e.g. [1, 2, 3, 4]), motivated by a range of areas of technological application, the structure of the thiolate/metal interface remains in doubt [5]. What seems to be clearly established is that for most of the alkylthiolates there are at least three distinct long-range ordered phases, namely a low coverage 'striped' of (m x $\sqrt{3}$) rect. phase (where m depends on the alkane chain length), in which the molecule is believed to 'lie down' on the surface, and two alternative high-coverage (0.33 ML) phases having ($\sqrt{3}$x$\sqrt{3}$)R30° and ($2\sqrt{3}$x3)rect.[†] periodicities, in which the molecules 'stand up', with a tilt angle of ~30° of the alkane chains relative to the surface normal. For the shortest chain length, methylthiolate (CH_3S-), there is no striped phase, and no convincing evidence of a ($2\sqrt{3}$x3)rect. phase.

By far the largest number of investigations of the thiolate/gold interface structure have been based not on experiments, but on density functional theory (DFT), and these are mostly of the simple Au(111)($\sqrt{3}$x$\sqrt{3}$)R30º-CH_3S phase for which intermolecular van der Waals interactions are expected to be relatively unimportant. Until quite recently almost all of these DFT studies concluded that the thiolate adsorbs onto an unreconstructed Au(111) surface with the S head-group atom in a three-fold or two-fold coordinated site; some studies favoured a hollow site [6, 7, 8, 9] (fig. 1), some a bridging site [10, 11, 12] (Fig. 2), and some a site displaced from the fully-symmetric bridge site towards the adjacent hollow [13, 14]. By contrast, two independent experimental studies of this surface phase, using entirely different experimental methods (S 2p photoelectron diffraction [15] and S 1s ionisation in normal-incidence X-ray standing waves (NIXSW) [16]), concluded that the S atom occupies atop sites (Fig. 1). A very recent near-edge X-ray absorption fine structure (NEXAFS) study has also led to the same conclusion regarding this local site [17], as has an investigation in which S 1s photoelectron

---

[†] The ($2\sqrt{3}$x3)rect. phase is referred to in much of the SAM literature as 'c(4x2)', though what is meant by this is actually c(4x2) relative to the ($\sqrt{3}$x$\sqrt{3}$)R30° mesh, not relative to the (1x1) substrate mesh. This nomenclature is inconsistent with standard practices of surface crystallography and will not be used here.

diffraction and NIXSW experiments were performed on the same surface preparations of this phase [18].

It now seems rather clear that the solution to this dilemma is that the creation of the thiolate overlayer leads to a reconstruction of the gold surface, though there is still no consensus as to the details of the reconstruction. This possibility had only been considered in one DFT study [19] until recently, but evidence of an adsorbate-induced reconstruction has emerged from recent experimental studies, and new DFT calculations do find some of these reconstructions to be energetically favourable. Scanning tunnelling microscope (STM) images at very low coverages have been interpreted in terms of the bonding of pairs of methylthiolate species to single Au adatoms to produce Au-adatom-dithiolate surface moieties [20]. The Au adatom is believed to occupy a bridging site on the underlying Au(111) surface with the S head-group atoms of the two thiolate species bonded to either side of this adatom such that they each lie atop Au atoms in the underlying surface (Fig. 2). The local ordering of this Au-adatom-dithiolate species, even at low coverages, is proposed to be consistent with the behaviour of long-chain alkylthiolates on Au(111) at low coverages when the alkyl chains are found to 'lie-down' on the surface, forming 'striped' phases. Evidence for similar Au-adatom-dithiolate species at low coverages has also been obtained by STM for phenylthiolate [21] and benzylthiolate [22]. Very recently, STM measurements at higher coverage have been interpreted as evidence that the Au(111)($\sqrt{3} \times \sqrt{3}$)R30º-CH_3S phase may actually be understood in terms of disordered layer of these Au-adatom-dithiolate species [21]. A rather different adatom reconstruction model has emerged from NIXSW studies of alkylthiolates of several different chain lengths at high (0.33 ML) coverage [23]. In particular, for the (2$\sqrt{3}$x3)rect. phase of hexylthiolate and octylthiolate the results indicate that the thiolate S headgroup atom occupies sites atop Au adatoms that are located in the two different hollow sites ('fcc' above third layer Au atoms, and 'hcp' above second layer Au atoms) on the surface. For the specific case of the Au(111)($\sqrt{3} \times \sqrt{3}$)R30º-CH_3S phase, this model would then imply that all the Au adatoms are in bulk-continuation ('fcc hollow') sites. This model thus involves Au-adatom-(mono)thiolate species in the hollow sites of the underlying Au(111) surface (Fig. 2).

3

An important feature of both of these adatom reconstruction models of the $(\sqrt{3}x\sqrt{3})R30^\circ$ phase is that the S head-group atoms of the thiolate are locally atop Au atoms in bulk-continuation sites. As such, both models of the $Au(111)(\sqrt{3}x\sqrt{3})R30^\circ$-$CH_3S$ phase could be consistent with previously published experimental data from photoelectron diffraction, NIXSW, and NEXAFS. Total energy calculations provide some support for both models [20, 24, 25], although they appear to favour the Au-adatom-dithiolate model, after taking account of the energy cost of creating the Au adatom. Recent molecular dynamics studies of the $Au(111)(\sqrt{3}x\sqrt{3})R30^\circ$-$CH_3S$ phase [26] and the $Au(111)(2\sqrt{3}x3)rect.$-$CH_3(CH_2)_5S$ phase [27] have concluded that these structures actually involve co-occupation of Au-adatom-dithiolate moieties and thiolate species bonded directly to the underlying surface with the S head-group atoms in bridging sites, together with a high degree of disorder. This picture appear to be consistent with surface X-ray diffraction (SXRD) data, although the experimental data were not tested against other structural models. In the case of the $Au(111)(\sqrt{3}x\sqrt{3})R30^\circ$-$CH_3S$ phase, the proposed structure was also claimed to be consistent with new experimental photoelectron diffraction [26], although the results of a subsequent combined NIXSW and photoelectron diffraction study specifically exclude any significant co-occupation of bridging sites [18], but fail to distinguish the different local atop models. The specific structural model derived in this way for the $Au(111)(2\sqrt{3}x3)rect.$-$CH_3(CH_2)_5S$ [27] also appears to be inconsistent with an analysis of the symmetry requirements imposed by systematic beam absences in surface SXRD and low energy electron diffraction (LEED) [28]. In summary, the Au-adatom-dithiolate model identified in STM images at low coverage is consistent with most photoelectron diffraction data and NIXSW measurements from $(\sqrt{3}x\sqrt{3})$ phases, and is supported by more recent theoretical calculations, but is inconsistent with NIXSW data from the $(2\sqrt{3}x3)rect.$ phases. By contrast, the Au-adatom-thiolate model accounts for all NIXSW data and is also consistent with photoelectron diffraction results, but is not favoured by theoretical total energy calculations, and cannot account for the low-coverage STM images.

In view of the continuing debate and apparent inconsistencies between the interpretation

of existing experimental and theoretical results, we have undertaken an investigation by an entirely different method, namely a study of the shifts in the Au 4f photoelectron core level binding energy from the Au(111) surface in different adsorption phases of methylthiolate and butylthiolate. The simple spectroscopic fingerprinting that underlies this study is clearly not able to provide quantitative surface structural information, but has the potential to identify the local coordination site of an adsorbate on a surface in a qualitative fashion. A particularly simple and elegant method of this kind, typified by experiments on the Rh(111)/CO adsorption system [29], involves investigation of the core-level binding energy shifts in photoemission from the substrate atoms. It is well known that photoemission from the atoms in the surface layer(s) of an elemental solid may show a different core-level binding energy than emission from atoms in the bulk due to differences in the structural and electronic environment. Moreover, if a surface atom is bonded to an adsorbate species, a different core-level shift (CLS) is observed. Predicting the magnitude and sign of these shifts is not generally trivial, because they derive from a combination of initial and final state effects: shifts in the one-electron binding energy in the initial ground-state atom, and changes in the interatomic relaxation energy in the ionic final state. However, these shifts provide a spectral fingerprint of the differently-bonded surface atoms, and the relative intensities of their associated photoemission peaks can be directly related to their relative occupancy on the surface. Thus, in the case of Rh(111)($\sqrt{3}$x$\sqrt{3}$)R30°-CO [29], for example, one can readily distinguish between CO adsorption in the three-fold-coordinated hollow sites, which would lead to all surface Rh atoms being bonded to CO and therefore none showing the core-level shift of the clean surface, and atop adsorption in which one third of the surface Rh atoms are bonded to CO and the remaining two thirds retain a core-level shift characteristic of the clean surface. Fig. 1 shows a diagram illustrating the equivalent structural models for two simple adsorption sites of methylthiolate adsorbed on (unreconstructed) Au(111). The existence of a resolvable surface component of the Au 4f photoemission signal from Au(111) is well-established (being one of the very first such surface-shifted peaks to be detected [30]), so a clear effect associated with the adsorption of thiolates can be expected and, indeed, is found, as reported here.

In a recent publication we have reported the main findings of these experiments for the specific case of the Au(111)($\sqrt{3}$x$\sqrt{3}$)R30º-CH$_3$S phase [31]. Here we provide fuller details of this investigation including data on the coverage dependence of the photoemission spectra, and present the results of a parallel investigation of Au(111)/CH$_3$(CH$_2$)$_3$S in both lying-down and standing-up ordered phases. We also discuss in more detail the implications of different structural models.

2. Experimental Details

The experiments were conducted on the beamline MPW6.1 of the Synchrotron Radiation Source at the CLRC's (Central Laboratories for the Research Councils) Daresbury Laboratory. This beamline has been described in detail elsewhere [32]; the source is a multi-pole wiggler and is fitted with a grazing incidence grating monochromator and a surface science end-chamber equipped with the usual *in situ* sample preparation and characterisation facilities. A concentric hemispherical analyser (with the axis of the entrance lens at 60° to the incident photon beam in the horizontal plane) was used to measure the energy distribution curves (EDCs) of photoemitted electrons at fixed pass energy. The Au(111) crystal sample was cleaned *in situ* by the usual combination of argon ion bombardment and annealing cycles to produce a clean well-ordered (22x$\sqrt{3}$)rect. 'herring-bone' reconstructed surface as assessed by the synchrotron radiation X-ray photoelectron spectroscopy (XPS), Auger electron spectroscopy, and LEED. Both the methylthiolate and butylthiolate surface species were formed by exposure of the clean surface to partial pressures of the vapour of the respective disulphides, dimethyldisulphide (DMDS - CH$_3$S-SCH$_3$) and dibutyldisulphide (DBDS - CH$_3$(CH$_2$)$_3$S-S(CH$_2$)$_3$CH$_3$); this avoids the use of the highly toxic methanethiol gas, while for the longer alkane chain species in particular it seems that S-S bond scission of the disulphide on Au(111) is more facile than deprotonation of the thiol at higher coverages. Typical exposures to obtain the saturation (0.33 ML) phases were explored in the range 8-1000 $\times$ 10^{-6} mbar.s with the sample at room temperature. S 1s XPS measurements showed these exposures led to saturation coverage, whilst LEED showed the expected ($\sqrt{3}$×$\sqrt{3}$)R30° pattern for methylthiolate. In the case of butylthiolate adsorption,

saturation also led to a diffraction pattern showing the $1/3^{rd}$ order diffracted beams characteristic of a $(\sqrt{3}\times\sqrt{3})R30°$ phase, but in general it was also possible to detect the additional beams associated with the $(2\sqrt{3}\times3)$rect. phase; we have found that these additional beams are generally most pronounced if the sample is cooled below room temperature [28]. It is well-established that for the longer-chain thiolates on Au(111) there is a co-existence of the $(\sqrt{3}\times\sqrt{3})R30°$ and $(2\sqrt{3}\times3)$rect. phases, and as the $1/3^{rd}$ order beams of the $(\sqrt{3}\times\sqrt{3})R30°$ phase are present for both phases, there is no simple way of quantifying the relative occupation of the two phases from LEED observations. It is also unclear whether the enhanced intensity of the $(2\sqrt{3}\times3)$rect. beams at lower temperatures is due to a change in the relative occupation of the two phases, or simply a consequence of the temperature dependence of the Debye-Waller factor. For the butylthiolate system, reduced exposures of DBDS, typically $\sim1x10^{-6}$ mbar.s, led to a $(12 \ x\sqrt{3})$rect. LEED pattern, characteristic of a lying-down or striped phase.

All photoemission spectra were recorded using normal incidence, the photoelectron detection angle thus being 60° from the surface normal, a geometry that enhances the surface specificity of the measurements. Measurements were made in two separate periods of beamtime allocation and the azimuthal orientations of the incidence plane in these two sets of experiments were 5° from <110>, and 9° from <211>, respectively. For the Au 4f measurements a photon energy of 135 eV was used, leading to a photoelectron kinetic energy of ~50 eV, a value close to the minimum in the 'universal curve' of attenuation lengths, further enhancing surface specificity. The low photoelectron energy also ensures that the electron energy analyser can be operated at high spectral resolution. Regular measurements were also made of the Fermi level cut-off region of the valence spectra to provide a more reliable energy reference for the measured binding energies. S 2p photoemission spectra were recorded for each surface preparation (at a photon energy of 210 eV) to provide an estimate of the relative thiolate coverage and to check for any indications of multiple adsorption states. Consistent with earlier reports [33], only a single S 2p photoelectron binding energy value was observed, independent of coverage.

3. Results

Fig. 3 shows the Au $4f_{7/2}$ photoemission spectrum from the clean Au(111) surface. The shape of this peak clearly indicates that there are (at least) two spectral components, and previous studies have found this spectrum can be fitted to two peaks, one attributed to emission from the surface layer of the clean surface, S_C, the other to emission from the underlying bulk material, B. Fig. 3 also shows such a fit, achieved using the computer program FitXPS2 [34], each component peak being described by a Doniach-Sunjic lineshape, convoluted with Gaussian functions, while a low-order polynomial is used to describe the background. The binding energy shift of the surface component is -0.34±0.02 eV relative to that from the bulk, in perfect agreement with the original report of this surface CLS which gave a value of -0.35 eV [30], and very close to the value of -0.31 eV found in a more recent high-resolution study [35]. The absolute value of the binding energy of the Au $4f_{7/2}$ bulk component is shown fixed in Fig. 3 at 84.00 eV; small variations in this value (mostly ~0.10 eV or less) in a number of measurements were seen, but may be due to limitations in exactly defining the location of the Fermi level or to calibration drift in the electron spectrometer. A striking feature of this spectrum is the fact that the surface component is actually more intense than that of the underlying bulk, unlike early reports of similar measurements [30]. This can be attributed to the particularly high surface specificity of our measurements conditions; the measured intensity ratio of the surface and bulk peaks in this spectrum is 2.67, implying an entirely reasonable value of the attenuation length of 6.5 Å. The spectral fit of Fig. 3 is achieved using a slightly larger value of the overall width of the surface peak than of the bulk peak, the FWHM (full-width half-maximum) values being 0.48 eV and 0.43 eV respectively. It is unclear whether this difference is due to the Lorentzian or Gaussian contributions. This same effect and the uncertainty in fitting has been reported in a detailed study of Al 2p emission from Al(111), the enhanced width of the surface component being attributed to a combination of crystal field splitting and inhomogeneous broadening to be expected at an imperfectly-ordered surface [36]. A reasonable (but less good) fit to the experimental spectrum of Fig. 3 can be achieved using two peaks with the same width parameters, but relaxing this constraint does improve the fit significantly, and also appears to have a

reasonable physical basis.

Fig. 4 shows a set of Au 4f photoemission spectra recorded from the Au(111) surface after deposition of increasingly higher coverages of methylthiolate. The coverage is estimated from the relative intensities of the S 2p and Au 4f photoemission peaks, assuming a calibration value of 0.33 ML for the highest coverage which displayed a ($\sqrt{3}$x$\sqrt{3}$)R30º LEED pattern. For the lowest two coverages the LEED pattern still showed the groups of diffracted beams around the (1x1) beams associated with the (22x$\sqrt{3}$)rect. reconstruction of the clean Au(111) surface, indicating that some parts of the surface retained the herring-bone reconstruction. It is well-established that quite low thiolate coverages lift this reconstruction (e.g [20]). These spectra show clearly that with increasing thiolate coverage the contribution from the highest kinetic energy (S_C) peak is reduced, while a new peak with a kinetic energy smaller than, but closer to, that of the bulk component, grows in intensity. What is also clear, though, is that at least the spectra corresponding to the higher coverages clearly also contain a component with a higher kinetic energy than that of the bulk component; i.e., these higher-coverage spectra clearly contains (at least) three distinct components with different associated binding energies. This general behaviour can be reconciled with the simple ideas that underlie the core-level-shift investigation of CO on Rh(111) [29] mentioned in the introduction. In particular, the simplest expectation for the spectrum from the adsorbate-covered surface is that it comprises three components, from Au atoms in the bulk (B), from Au atoms in the surface that are bonded to the thiolate species (T) and from Au atoms in the surface that are not bonded to the thiolate species, (S). Notice that the fact that the clean Au(111) surface is reconstructed, but that this reconstruction is lifted by the surface thiolate species, means that we might expect different photoelectron binding energies for the Au atoms in the clean reconstructed surface from those that are not bonded to thiolate species in the thiolate-covered surface. For this reason the surface component from the clean reconstructed surface is distinguished as S_C .

This rationale indicates, of course, that at the lowest thiolate coverage the uppermost spectra of Fig. 4 corresponding to low thiolate coverages should actually contain four

contributions, B, T, S, and S_C. However, the S and S_C components only differ in binding energy by approximately 0.1 eV, so while four-peak fits to a range of spectra recorded at low and medium coverages of thiolate were possible, it proved difficult to draw consistent and reliable conclusions from such fits regarding the relative energies and intensities of all the components. Three-component fits to most spectra, and particularly to those corresponding to the ordered ($\sqrt{3}$x$\sqrt{3}$)R30° phase, did prove very stable over a large number of spectra recorded for different preparations, although in these fits the surface component energy shift changed slightly from the S_C value of -0.34 eV to the S value of -0.23 eV with increasing thiolate coverage in the range up to ~0.05-0.10 ML, corresponding to the expected transfer of intensity from an S_C component to an S component. Note that while there is no simple way of predicting the value of these surface core-level shifts, the fact that the sign of the shifts associated with the S_C and S peaks is the same is consistent with the standard models of their origin [37].

Examples of Au 4f spectra from the ($\sqrt{3}$x$\sqrt{3}$)R30°-CH$_3$S phase are shown in Fig. 5; the left and right-hand panels show two different experimental spectra, while the upper and lower fits are achieved using different constraints. The assignment of the T and S components to the lowest and highest kinetic energy peaks is based on the results of fitting spectra at intermediate coverages; at the lowest thiolate coverages a very small T peak is found, while the binding energy of the single S peaks is essentially identical to that of the S_C peak. At only slightly higher coverages the binding energy of the S peak stabilises at a different value, corresponding to the value found for the ($\sqrt{3}$x$\sqrt{3}$)R30° phase, while the T peak intensity grows with increasing thiolate coverage. In fitting complex peak shapes to several components that are not clearly resolved it is, of course, generally important to apply some constraints. Unconstrained fits can always be achieved, and the lack of constraints generally means the fit quality is better, but their physical significance may be questionable. The constraints applied in obtaining the upper pair of fits in Fig. 5 are that the width and absolute binding energy (to within a few meV) of the B peak should be identical to those of the B peak in the clean surface spectrum, while the widths of T and S peaks should be the same as that of the S_C peak obtained from the clean surface. Using this procedure led to consistent relative binding energies of the

10

components, not only for data from the preparations of the (√3x√3)R30º phase, but also from all other preparations other than those at very low coverage, for which some component from the herring-bone reconstructed clean surface (and thus a contribution from a S_C peak) may be anticipated. The core-level binding energy shift values, relative to that of the bulk component, resulting from these fits to a large number of different spectral measurements from separate surface preparations, were -0.23±0.02 eV for the S peak and +0.34±0.02 eV for the T peak. For the ordered (√3x√3)R30º phase spectra, the relative intensities (defined by the peak areas) of these two peaks, S:T, was 3.1±0.2. The structural implications of this value are discussed in section 4. These fits led to a surface-to-bulk peak intensity ratio, S+T:B of 2.7±0.1, closely similar to that of the clean surface.

Also shown in the lower parts of Fig. 5 are alternative three-component fits to the same experimental spectra in which the constraints on the peak width parameters have been relaxed. Somewhat improved fits are obtained (as reflected by the residuals). The relaxed constraints giving rise to these new fits led to a consistent increase in the width of the T peak by 0.12 eV and this was accompanied by changes in the ratio of the peak intensities, with new values for S:T of 2.2±0.2 and for S+T:B of approximately 2.2. The relative component binding energies are essentially identical to those of the constrained fits. A key question, of course, is whether this improved fit is meaningful, or simply reflects the fact that one can always improve a fit by increasing the number of fitting parameters. One rather general problem with this solution is that it is difficult to understand why the ratio of the intensity of emission from surface atoms relative to that from the underlying bulk should be substantially reduced as a result of the thiolate adsorption. There is, of course, also a question as to why the T peak should be significantly broader that the S peak; we will address these questions in considering specific structural models in the following section.

The Au 4f photoemission measurements from the butylthiolate adsorbate layers produced essentially identical results in the number of component peaks, their energy separation, and their relative intensities at saturation coverage. Fig. 6 shows two example fits. For the saturation coverage experiments there was no obvious difference between surfaces

appearing to show only ($\sqrt{3}$x$\sqrt{3}$)R30º ordering and those displaying the extra diffracted beams of the (2$\sqrt{3}$x3)rect. phase. Because of the commonality of the($\sqrt{3}$x$\sqrt{3}$)R30º diffracted beams to both phases this may be simply because the fractional occupation of the (2$\sqrt{3}$x3)rect. is low, although it could also be that the local geometry is, from the point of view of the photoemission, essentially the same in both phases. The one key difference between the methylthiolate and butylthiolate adsorption systems, of course, is the existence of the lower-coverage striped phase in which the alkane chains are more nearly parallel to the surface, and one objective of our measurements was to try to also identify the local interface structure in this phase. Unfortunately, measurements from several different surface preparations, each showing the (12x$\sqrt{3}$)rect. LEED pattern characteristic of this phase, led to very large variations in the $S{:}T$ intensity ratio in the range ~5-10. Indeed, in the spectra yielding the highest value of this ratio, it was notable that the core level shift associated with the nominal S peak was actually quite close to the value found for the S_C clean surface value. The implication is that islands of the striped phase may form at sufficiently low average values of the coverage that regions of the clean surface herring-bone reconstruction are still present. Moreover, the fact that the LEED pattern of the (three rotational domains of the) (12x$\sqrt{3}$)rect. phase contains 1/3rd order beams at the same locations as those that characterise the ($\sqrt{3}$x$\sqrt{3}$)R30º phase, means that unidentified coexistence of these two phases may also arise (at higher coverages). We conclude, therefore, that it is not possible to reliably relate any particular Au 4f spectrum to a surface that corresponds to a fully saturated (12x$\sqrt{3}$)rect. phase with no significant amount of coexistent clean surface or ($\sqrt{3}$x$\sqrt{3}$)R30º phase. By contrast, of course, the fact that the ($\sqrt{3}$x$\sqrt{3}$)R30º (and (2$\sqrt{3}$x3)rect.) phases of the two adsorbates correspond to the same saturation coverage, means that the results obtained from these phases are not influenced by problems associated with variable coverage, as reflected in the small scatter of the parameters extracted from many different surface preparations.

4. Discussion

From the point of view of providing information on the thiol/metal interface structure, the key experimental result is the $S{:}T$ intensity ratio for the saturation coverage phases of the

two thiolates. For the ordered $(\sqrt{3}x\sqrt{3})R30°$ phase, with one thiolate species per surface unit mesh, the expected results of the CLS experiment are clear for most of the simple structural model. In particular, if the thiolate adsorption is on an unreconstructed (1x1) Au(111) surface (as in Fig. 1), then simple counting of surface atoms leads one to expect the following S:T intensity ratios for the different high-symmetry adsorption sites: hollow, 0:3 (i.e. in this case there is no S peak, only B and T peaks); bridge, 1:2; atop, 2:1. It is also straightforward to show that for the Au-adatom-monothiolate structural model the expected ratio is 3:1. Application of these simple arguments to the Au-adatom-dithiolate model is less straightforward for two reasons. Firstly, it is not possible to form an ordered Au(111)$(\sqrt{3}x\sqrt{3})R30°$ phase with a coverage of 0.33 ML of thiolate species from the Au-adatom-dithiolate model; 0.33 ML of these moieties corresponds to 0.66 ML of thiolate species, so we must model this surface with an Au-adatom-dithiolate coverage of 0.16 ML, which we assume to adopt a (hypothetical) ordered $(2\sqrt{3}x\sqrt{3})R30°$ phase. Secondly, for this surface moiety, there are two different types of surface Au atom bonded to the thiolate species, namely the Au adatoms (bonded to two thiolate species) and the surface layer Au atoms directly below the thiolates. If we label these two Au atoms as T_{ad} and T_S, respectively, and note that the $(2\sqrt{3}x\sqrt{3})R30°$ unit mesh contains one Au adatom, two thiolate species, and four surface Au atoms that are not bonded to the thiolate, we find a ratio for S:T_{ad}:T_S of 4:1:2; if these two distinct types of Au bonded to thiolate have the same CLS the S:T ratio would be 4:3. Of course, the fact that it is not possible to form an ordered Au(111)$(\sqrt{3}x\sqrt{3})R30°$ phase with a coverage of 0.33 ML of thiolate species from the Au-adatom-dithiolate model appears to lead to a fundamental contradiction with the observed diffraction patterns, but it has been suggested that this apparent contradiction may be due to a high degree of disorder [26], and the very recent STM results provide some direct support for this contention [21].

The experimentally measured value of the S:T ratio obtained in the preferred constrained fits of the methylthiolate data of 3.1±0.2 is clearly compatible only with the Au-adatom-monothiolate structural model. The fact that the same S:T ratio is found for the butlythiolate data, implies that this species also adopts this same structure. Note that the NIXSW study which led to the original proposal of this model concluded that for the

longer-chain thiolates the only difference between the structures of the (√3x√3)R30°
phase and the (3x2√3)rect. phase was in the relative occupation by the Au adatoms of the
fcc and hcp hollow sites; the predicted S:T ratio is the same for these two sites, so the
relative occupation of these two phases has no influence on this interpretation. The
unconstrained spectral fit, which we have been inclined to discard on the basis of the
change in the surface-to-bulk intensity ratio relative to the clean surface (as discussed
above), leads to a value of the S:T ratio closer to 2, which would imply atop adsorption
on an unreconstructed surface. The fact that this model is inconsistent with other
experimental and theoretical data would seem to add to the reasons to reject this fitting
solution.

While the measured S:T ratio of 3.1±0.2 from the constrained experimental fit is clearly
inconsistent with the value of 1.33 deduced for the Au-adatom-dithiolate model, this
value was obtained on the assumption that the T_S and T_{ad} surface Au atoms should have
the same photoelectron binding energy. As it is far from certain that this would be the
case, it is important to re-examine this issue. The anticipated ratio of peak intensities
based on a four-component solution has already been given above, namely S:T_{ad}:T_S
should be 4:1:2. The fact that we obtain a good fit with only two surface components
presumably implies that if there are really three surface components, the energy
difference between two of these three components must be small. So far we have
assumed that these are the T_S and T_{ad} components, and indeed this interpretation would be
consistent with an increase in the spectral width of the T peak as found in the
unconstrained fit to the experimental spectra, but the experimental S:T ratio of 2.2±0.2
obtained in this unconstrained fit is still very different from the predicted value of 1.33.
Are there other possible peak overlaps that could account for the data? The alternative
interpretations are that one of the two T components could overlap with the S peak.
Neither possibility, however, is consistent with our data. The predicted $S+T_{ad}$:T_S ratio
would be 6:1, clearly incompatible with the experimental data. The $S+T_S$:T_{ad} ratio would
be 5:2 – i.e. 2.5 – not too different from the value we obtain for our unconstrained fit to
the data, but in this interpretation it is the S peak, now assigned to a combination of the S
and T_S components, and not the T peak, as observed, that would be expected to be

14

slightly broader due to the two contributing components.

So far, throughout this discussion, we have assumed that there is a linear relationship between the integrated intensities of the surface-related photoemission peaks and the relative number of such atoms on the surface. One effect which could invalidate this assumption is the role of photoelectron diffraction. The coherent interference of the directly-emitted component of the photoelectron wavefield from a surface adsorbate atom with other components elastically backscattered by the underlying substrate atoms is an established method for determining the adsorption geometry, and in favourable circumstances modulations in the intensity of as much as 50% may be detected as a function of photoelectron energy or direction [38, 39]. Similar effects can occur for emission of outermost surface layer substrate atoms due to scattering by the underlying substrate. Thus, if one has Au emitter atoms in very different local geometries, there could be significant differences in the measured intensity at a specific energy and direction due to photoelectron diffraction. Indeed, Cossaro *et al.* have recently highlighted the potential role of photoelectron diffraction in the systems studied here [40, 41]; they have presented similar Au 4f spectra from the Au(111)($\sqrt{3}$x$\sqrt{3}$)R30°-CH$_3$S surface recorded at normal emission and at 60° polar emission angle and show that there is a very significant difference in the *S*:*T* ratio for these two measurements, an effect they attribute to photoelectron diffraction. While this attribution is almost certainly correct, there are several reasons for believing that photoelectron diffraction is unlikely to have a significant influence on the data presented here. In particular, the strongest photoelectron diffraction effects are generally found in highly-symmetric emission directions, typically in normal emission or in near-neighbour interatomic directions that correspond to favoured 180° backscattering. The present measurements, however, were made in low symmetry azimuths at a polar emission angle of 60°, far from normal emission. Moreover, the data were collected in two separate sets of experiments in distinctly different azimuthal directions of electron collection, yet there is no discernible difference in the spectral fits obtained in these measurements, nor in their associated *S*:*T* intensity ratios. It is possible that measurements in more high-symmetry directions would have yielded some differences in intensity ratios, but our measurement geometries appear to

15

correspond to conditions in which the influence of photoelectron diffraction is minimal.

The other key assumption of our analysis is that the surface is well-ordered, although there is some indirect evidence from X-ray diffraction and molecular dynamics [26], and direct evidence from STM (albeit imaged at 5K) [21] that the saturation phase of methylthiolate is not well ordered. How may this influence the interpretation of our results? Perhaps the most obvious influence is that, as near-neighbour intermolecular distances are unlikely to be reduced below that expected of the ordered phases, disorder will lead to reduced coverage, increasing the number of surface Au atoms that are not bonded to thiolate species. This will cause an increase in the S:T ratio by an amount that depends on the coverage and the particular structural model. In their modelling of the disordered Au-adatom-dithiolate structure seen in STM, Voznyy *et al.* consider a structure with only 75% of the saturation coverage of the fully-ordered structure. Such a coverage from this model would lead to a significant increase in the S components. Specifically, we have argued that in a (hypothetical) ordered $(2\sqrt{3}\times\sqrt{3})R30°$ phase there are 4 S atoms and 3 T atoms per unit mesh. On the bare areas of a disordered surface, however, there are 6 S atoms per unit mesh, so if only 75% of the surface is covered, the S:T ratio would increase from 4:3 on the ordered surface to $(4+(6/3))$:3 or 2:1, a value that could now be reconciled with the unconstrained fits to the experimental spectra. Moreover, the fact that the T peak would actually comprise two distinct components, T_{ad} and T_S would provide a rationale for the increased spectral width of the T peak. This interpretation, however, fails to account for the changed bulk-to-surface peak ratio produced by the unconstrained fits.

While the study reported here appears to be the first one that attempts to identify thiolate adsorption sites on the Au(111) surface from the Au 4f photoemission spectra, it is certainly not the first measurement of such data. Most relevant is a study of thiolate-induced changes in Au 4f photoemission from longer-chain alkylthiols on Au(111). In the case of dodecanethiol on Au(111), the Au 4f spectrum after dosing appeared to show a strong shift of the surface component to within 0.06 eV of the bulk peak, but only a weak shoulder on the high binding energy side that might relate to the T peak seen in our

measurements [35]. The shape of these spectra is thus quite different from those reported here. It is known, of course, that the longer chain thiolate layers show a much stronger influence of the (2√3x3)rect. phase, whereas for methylthiolate this phase is absent, and even for butylthiolate the (√3x√3)R30° phase is probably dominant. The implication is therefore that there is a fundamental difference in the local structure (or at least of the interface electronic structure) within the (2√3x3)rect. and the (√3x√3)R30° phases. There have also been measurements of the effect of longer-chain thiolate adsorption on small Au particles. In this case adsorption appeared to quench the surface component (presumably because, in this case too, the modified surface component overlaps that of the bulk), with the appearance of a thiol-related peak at higher binding energy than the bulk component; no multi-component analysis of these complex adsorbate-covered surfaces was undertaken [42].

The fact that adsorption of longer-chain alkylthiolates causes the S peak to adopt a photoelectron binding energy essentially identical to that of the bulk does raise one further question. Could it be that this is also true for methylthiol and butylthiolate, and that the peak assignments are incorrect? For example, the peaks assigned to S and T could really be the expected T_S and T_{ad} components expected for the Au-adatom-dithiolate model with an intensity ratio of 2:1, as found in the unconstrained peak fitting, while the decreased surface-to-bulk intensity ratio of this fit could be due to the overlap of the S and B components. However, a simple calculation shows that this would lead to far too much intensity being transferred to the bulk peak, with a predicted surface-to-bulk ratio, $(T_S + T_{ad})$:$(B+S)$ of only 0.32, to be compared with an experimental value of 2.2.

5. Conclusions

Measurements of the Au 4f photoemission spectrum from Au(111) as a function of coverage of methylthiolate or butylthiolate show essentially identical behaviour. The clean surface spectrum can be clearly reconciled with two components at different photoelectron binding energies, consistent with emission from atoms in the bulk and atoms in the reconstructed surface layer, as previously reported by several groups. With

increasing thiolate coverage the surface component (at lower binding energy than that of the bulk emission) shifts slightly in energy towards the bulk binding energy, while a new component grows at higher binding energy. The shift in the surface component can be attributed to the thiolate-induced lifting of the herring-bone reconstruction of the surface layer, while the higher binding energy component is assigned to emission from surface Au atoms bonded to thiolate species. The intensity ratio (3.1±0.2) of these new surface components at saturation coverage, fitted by peaks of identical spectral width, is found to be consistent with only one structural model of a well-ordered surface, namely thiolate adsorption atop individual Au adatoms. If the parameters of the spectral fitting are relaxed to allow different widths to the component peaks, the intensity ratio falls to 2.2±0.2, but there is also a 20% decrease in the surface-to-bulk ratio relative to the value of the clean surface. The revised intensity ratio of the two surface-related components would imply a model involving atop adsorption on an unreconstructed surface but such a model is not only inconsistent with a significant amount of evidence of Au adatom reconstruction from other experiments, but also provides no rationale for the modified surface-to-bulk peaks ratio. Our results thus appear to clearly favour the Au-adatom-thiolate model over the Au-adatom-dithiolate model.

We note, however, that the recent STM study of Voznyy *et al.* [21] leads to a structural model of the surface, based entirely on Au-adatom-dithiolate species, that involves a high degree of disorder. If this were to result in a decrease of the thiolate coverage to 75% of the saturation value for an ordered phase, this model could account for our measured ratio of the intensities of the two surface-related spectral peaks, although not for the reduced surface-to-bulk intensity ratio. Ultimately these ambiguities may only be resolved by a fully quantitative assignments of the different core-level-shifted spectral components through proper calculations of the expected shifts for the different structural models. Such calculations must, of course, include both initial and final state effects in the photoemission.

One striking feature of the photoemission data presented here (and reproduced in independent measurements by Cossaro *et al.* [40]) is a qualitative difference between the

these data from short-chain alkylthiolates, and spectra from longer-chain species previously studied by others [35]. While there is clearly a difference in the long-range ordered phases, mainly (2√3x3)rect. for the longer molecules and (√3x√3)R30° for the shorter ones, it has generally been assumed that the local interface structures have much in common. These data appear to cast some doubt on this view.

Acknowledgements
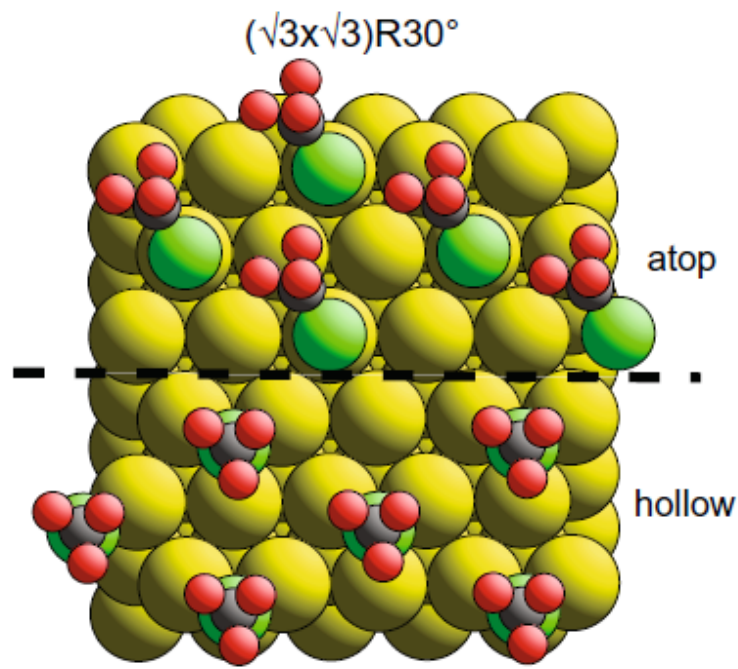
Fig. 1 Schematic plan view of the Au(111) surface showing two possible arrangements of methylthiolate species on the surface in ordered ($\sqrt{3} \times \sqrt{3}$)R30º phases based on adsorption in local atop and hollow sites on an unreconstructed metal surface.
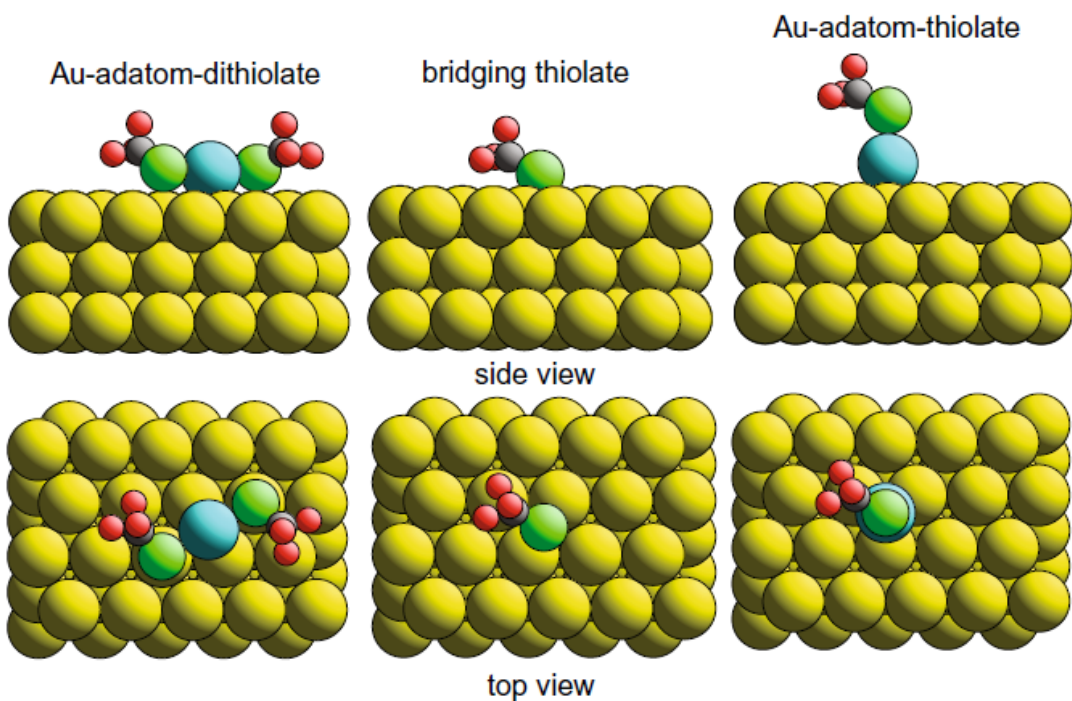
Fig. 2 Schematic side views of the two recently-proposed Au adatom reconstruction models for the Au(111)/methylthiolate surface, and the bridging thiolate species on the unreconstructed surface. On the left is shown the Au-adatom-dithiolate model in which two thiolate species lie on either side of a bridge-bonded Au adatom with the S atoms in near-atop sites relative to the underlying Au(111) surface. On the right is shown the Au-adatom-thiolate model in which the thiolate lies atop an Au adatom which occupies a bulk-continuation fcc hollow site. In the centre is the simple bridging thiolate that has been proposed to coexist on the surface with the Au-adatom-dithiolate species.
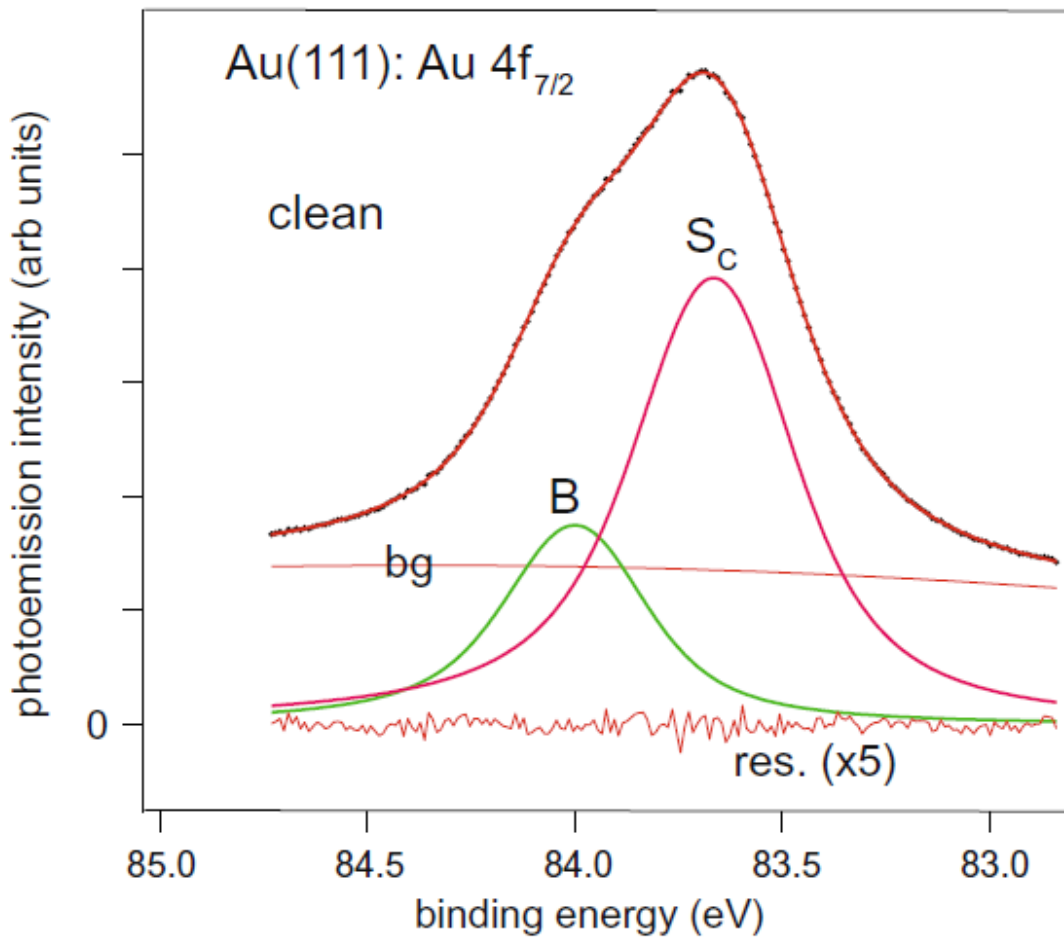
Fig. 3 Au $4f_{7/2}$ photoemission spectra from the clean Au(111)(22x√3)rect. surface. The upper spectrum is the experimental data (individual points) and the spectral fit (continuous line) made up of a sum of the individual components peaks from the surface atoms, S_C, and from the underlying bulk, B, and the background (bg). At the bottom is shown the residual in the fitting with an enhanced amplitude scale (x5).
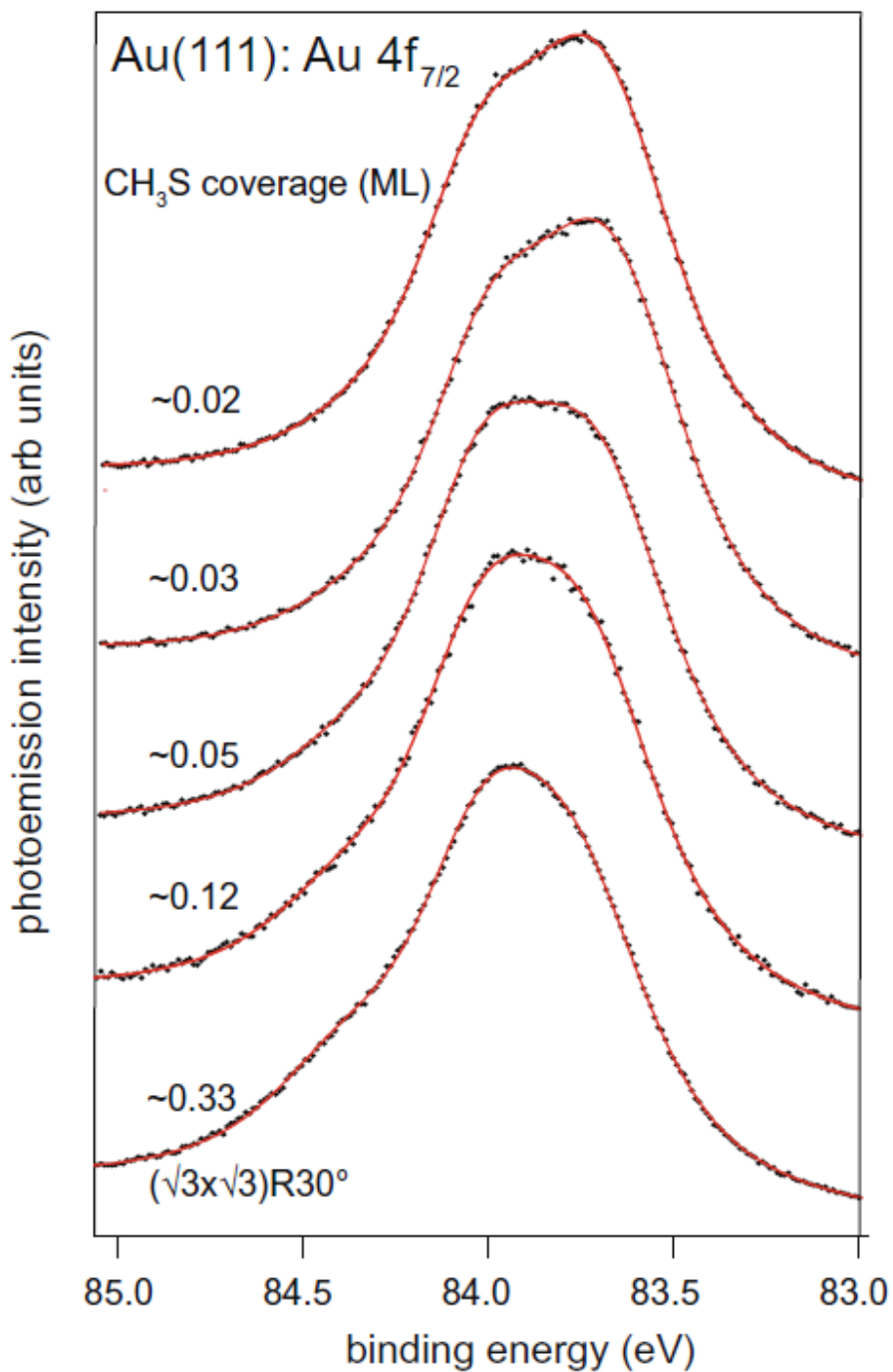
Fig. 4 Au $4f_{7/2}$ photoemission spectra from the Au(111) surface with different coverages of methylthiolate. The experimental data are shown as individual points while spectral fits are shown as continuous lines.

Au(111)(√3x√3)R30°-CH$_3$S: Au 4f$_{7/2}$
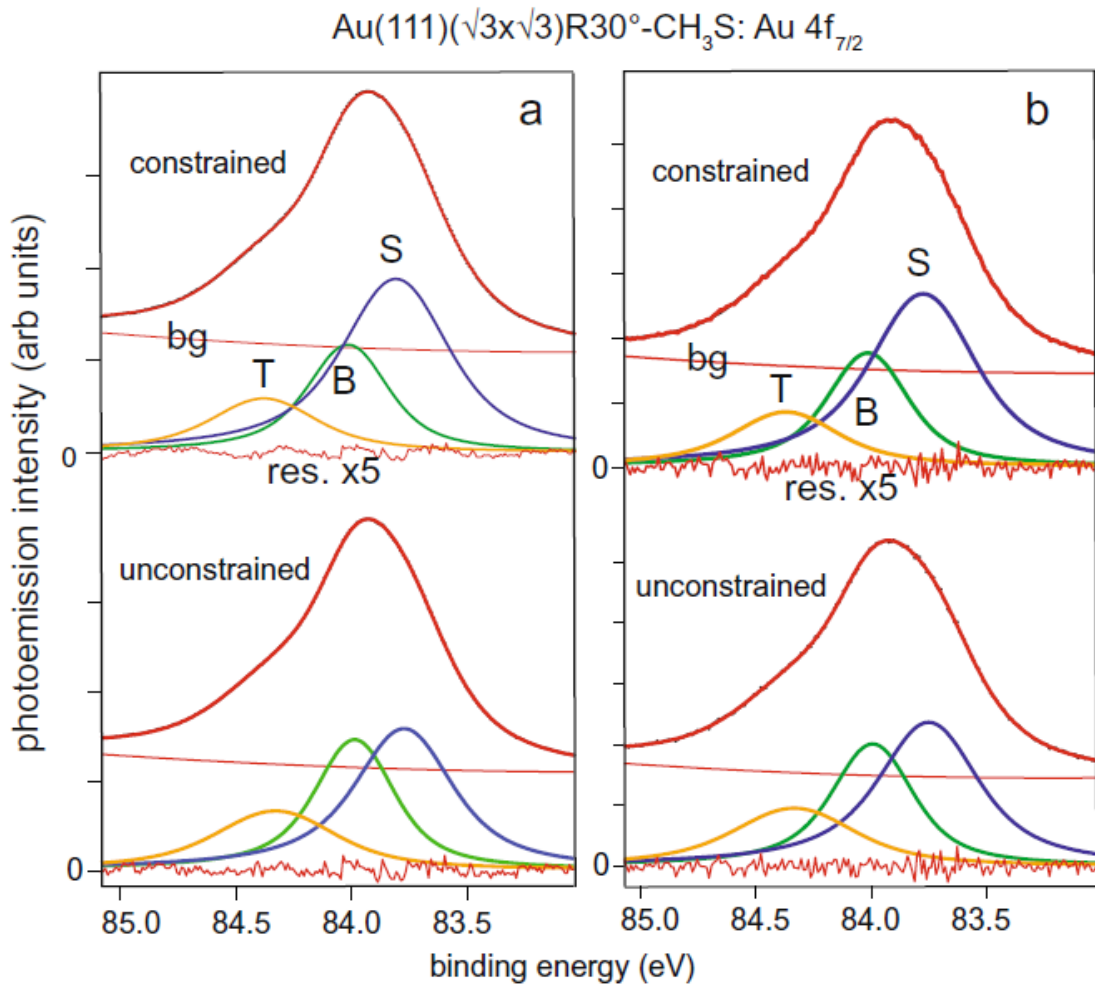
Fig. 5. Two different examples of Au 4f$_{7/2}$ photoemission spectra from the Au(111)(√3x√3)R30ºCH$_3$S adsorption phase. In each case the upper spectrum is the experimental data (individual points) and the spectral fit (continuous line) made up of a sum of the individual components peaks and the background (bg). At the bottom of each group is shown the residual in the fitting with an enhanced amplitude scale (x5). The upper pair of fits were conducted with the widths of the individual components constrained as described in the text; in the lower pair these constraints were relaxed.
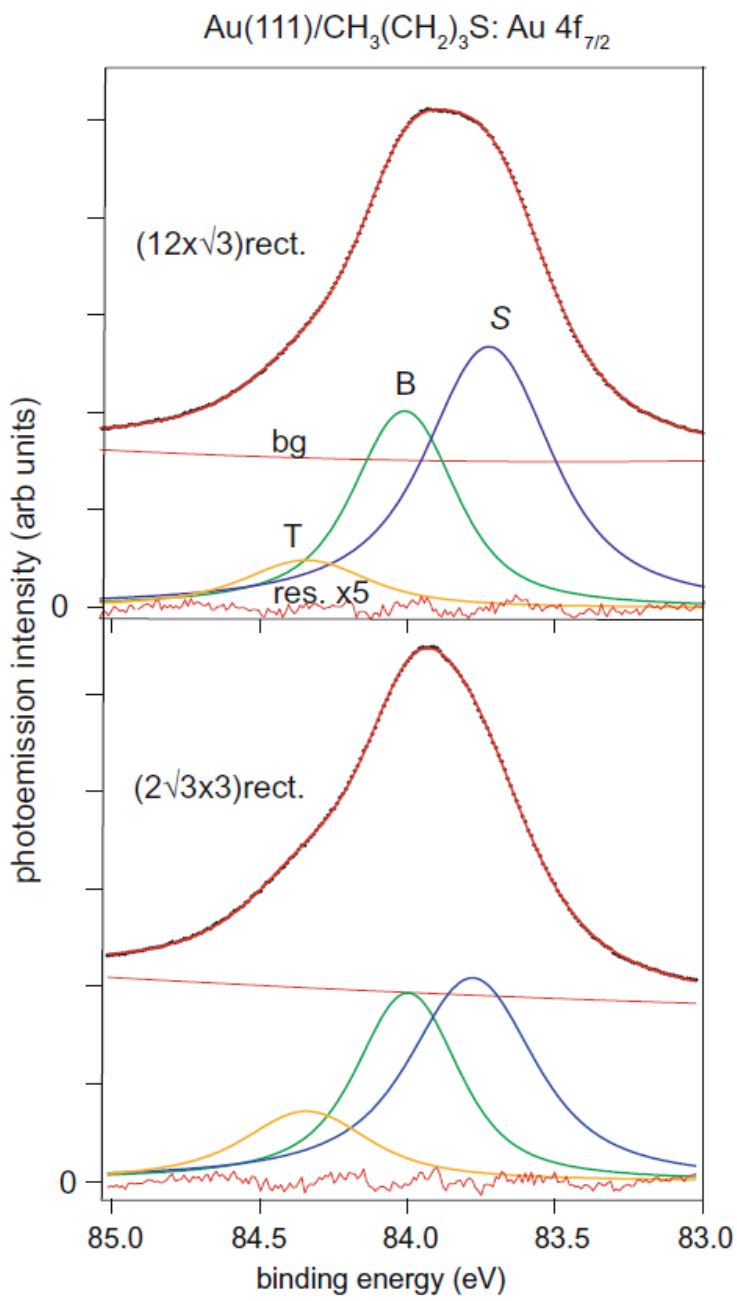
Fig. 6. Au $4f_{7/2}$ photoemission spectra from Au(111) surfaces with adsorbed butylthiolate displaying two different ordered LEED patterns. In each case the upper spectrum is the experimental data (individual points) and the spectral fit (continuous line) made up of a sum of the individual components peaks and the background (bg). At the bottom of each group is shown the residual in the fitting with an enhanced amplitude scale (x5).

References

1 L. H. Dubois, R. G. Nuzzo, Annu. Rev. Phys. Chem. 43 (1992) 437.

2 F. Schreiber, Prog. Surf. Sci. 65 (2000) 151.

3 A. Ulman, Chem. Rev. 96 (1996) 1533.

4 C. Vericat, M. E. Vela, R. C. Salvarezza, Phys. Chem. Chem. Phys. 7 (2005) 3258.

5 D.P. Woodruff, Phys. Chem. Chem. Phys. 10 (2008) 7211.

6 H. Sellers, A. Ulman, Y Shnidman, J.E. Eilers, J. Am. Chem. Soc., 115 (1993) 9389.

7 H. Gronbeck, A. Curioni, W. Andreoni, J. Am. Chem. Soc., 122 (2000) 3839.

8 Y. Yourdshahyan, H.K. Zhang, A.M. Rappe, Phys. Rev. B, 63 (2001) 081405.

9 M. Tachibana, K. Yoshizawa, A. Ogawa, H. Fujimoto, R. Hofmann, J. Phys. Chem. B, 106 (2002) 12727.

10 T. Hayashi, Y. Morikawa, H. Nozoye, J. Chem. Phys., 114 (2001) 7615.

11 M.C. Vargas, P. Giannozzi, A. Selloni, G. Scoles, J. Phys. Chem. B, 105 (2001) 9509.

12 J. Gottschalck, B. Hammer, J. Chem. Phys., 116 (2002) 784.

13 Y. Akinaga, T. Nakajima, K. Hirao, J. Chem. Phys., 114 (2001) 8555.

14 Y. Morikawa, T. Hayashi, C.C. Liew, H. Nozoye, Surf. Sci., 507-510 (2002) 46.

15 H. Kondoh, M. Iwasaki, T. Shimada, K. Amemiya, T. Yokohama, T. Ohta, M. Shimomura, K. Kono, Phys. Rev. Lett. 90 (2003) 066102.

16 M.G. Roper, M.P. Skegg, C.J. Fisher, J.J. Lee, V. R. Dhanak, D.P. Woodruff, R. G. Jones, Chem. Phys. Lett. 389 (2004) 87.

17 A. Chaudhuri, M. Odelius, R.G. Jones, T.-L. Lee, B. Detlefs, D.P.Woodruff, J. Chem. Phys. 130 (2009) 124708.

18 D.C. Jackson, A. Chaudhuri, T.J. Lerotholi, D.P. Woodruff, R.G. Jones, V. Dhanak, Surf. Sci. 603 (2009) 807.

19 M.L. Molina, B. Hammer, Chem. Phys. Lett., 360 (2002) 264.

20 P. Maksymovych, D. S. Sorescu, J. T. Yates, Jr. Phys. Rev. Lett. 97 (2006) 146103.

21 O. Voznyy, J.J. Dubowski, J.T. Yates Jr., P. Maksymovych, J. Am Chem. Soc. 131 (2009) in press (http://pubs.acs.org/doi/abs/10.1021/ja902629y).

22 P. Maksymovych, J. T. Yates, Jr., J. Am. Chem. Soc. 130 (2008) 7518.

23 Miao Yu, N. Bovet, Christopher J. Satterley, S. Bengió, Kevin R. J. Lovelock, P. K. Milligan, Robert G. Jones, D. P. Woodruff, V. Dhanak**,** Phys. Rev. Lett. 97 (2006) 166102.

24 F. P. Cometto, P. Paredes-Olivera, V. A. Macagno, E. M. Patrito, J. Phys. Chem. B 105 (2005) 21737.

25 H. Grönbeck and H. Häkkinen, J. Phys. Chem. B, 111 (2007) 3325.

26 R. Mazzarello, A. Cossaro, A. Verdini, R. Rousseau, L. Casalis, M.F. Danisman, L. Floreano, S. Scandolo, A. Morgante, G. Scoles, Phys. Rev. Lett., 98 (2007) 016102.

27 A. Cossaro, R. Mazzarello, R. Rousseau, L. Casalis, A. Verdini, A. Kohlmeyer, L. Floreano, S. Scandolo, A. Morgante, M.L. Klein, G. Scoles, Science, 321 (2008) 943.

28 A. Chaudhuri, T.J. Lerotholi, D.C. Jackson, D.P. Woodruff, R.G. Jones, Phys. Rev. B, 79 (2009) 195439.

29 A. Beutler, E. Lundgren, R. Nyholm, J.N. Andersen, B.J. Setlik, D. Heskett, Surf. Sci., 396 (1998) 117.

30 P. Heiman, J.J. van der Veen, D.E. Eastman, Solid State Commun. 38 (1981) 595.

31 A. Chaudhuri, T.J. Lerotholi, D.C. Jackson, D.P. Woodruff, V. Dhanak, Phys. Rev. Lett. 102 (2009) 126101.

32 M. Bowler, J.B. West, F.M. Quinn, D.M.P. Holland, B. Fell, P.A. Hatherly, I. Humphrey, W.R. Flavell, B. Hamilton, Surf. Rev. Lett. 9 (2002) 577.

33 M. Zharnikov, M. Grunze, J. Phys.: Condens. Matter 13 (2001) 11333.

34 D.L. Adams and J.N. Andersen: software can be downloaded at http://www.sljus.lu.se/download.html

35 K. Heister, M. Zharnokov, M. Grunze, L.S.O. Johansson, J. Phys. Chem. B. 105 (2001) 4058.

36 M. Borg, M. Birgersson, M. Smedh, A. Mikkelsen, D.L. Adams, R. Nyholm, C.-O. Almbladh, J.N. Andersen, Phys. Rev. B 69 (2004) 235418.

37 D.P Woodruff, T.A. Delchar, *Modern Techniques of Surface Science – Second Edition* (Cambridge University Press, Cambridge, 1994) pp 149-151

38 D. P. Woodruff, A. M. Bradshaw Rep. Prog. Phys. 57 (1994) 1029.

39 D. P. Woodruff, Surf. Sci. Rep. 62 (2007) 1.

40 A. Cossaro, L. Floreano, A. Verdini, L. Casalis, A. Morgante, Phys. Rev. Lett. 103
(2009) 119601

41 A. Chaudhuri, T.J. Lerotholi, D.C. Jackson, D.P. Woodruff, V. Dhanak, Phys. Rev.
Lett. 103 (2009) 119602

42 A. Tanaka, M. Imamura, H. Yasuda, Phys. Rev. B **74**, 113402 (2006).